

IMECE2002-33375

STUDY OF THE ACOUSTIC OSCILLATIONS BY FLOWS OVER CAVITIES.
PART 1. INTERNAL FLOWS

Xavier Amandolèse

Institut Aérotechnique
15, rue Marat

F-78210 Saint-Cyr l'Ecole, France

E-mail : xavier.amandolèse@iat.cnam.fr

Pascal Hémon

Institut Aérotechnique, now at
Hydrodynamics Laboratory – LadHyX

Ecole Polytechnique - CNRS

F-91128 Palaiseau, France

Clotilde Regardin

Institut Aérotechnique

15, rue Marat

F-78210 Saint-Cyr l'Ecole, France

Keywords : aeroacoustics, cavity, resonator, shear layer, instability

ABSTRACT

We present a study of acoustic oscillations induced by an internal airflow over a shallow and a deep cavity. The Kelvin-Helmholtz instability is interacting with an acoustic mode of the duct, leading to a resonance which produces a very high sound level. The influence of upstream boundary layer thickness and neck thickness is studied. Some results obtained by modifying the upstream lip shape, by crenel addition, are also given. It is also shown that the numerical simulations using a lattice-gas method give relatively good results by comparison with the experiments. Especially the resonance with the duct acoustics was qualitatively reproduced.

INTRODUCTION

The problem deals with the internal flows encountered in many industrial processes where a fluid has to be transported in a piping system. All the valves or other elements may create a flush mounted cavity as presented in Figure 1. The shear layer usually exhibits a periodic vortex organization that can interact with some eigenmodes of the system, particularly the volume of the cavity, creating a so-called Helmholtz resonator, or an acoustic mode of the duct. This paper deals mainly with the interactions of the duct with a deep and a shallow cavity. The Helmholtz resonator, similar to the phenomenon occurring in car vehicles with an open roof, is detailed in part 2 of the paper, Hémon et al. (2002), where a semi-active sound reduction system is proposed.

The problem of shear layer instability has been widely studied in various situations, Ho & Huerre (1984). Particularly,

the impinging shear layers are known to be responsible for coherent oscillations when the wave length associated to the vortices is close to the neck length L (see Figure 1), Ziada & Rockwell (1982), Rockwell (1983).

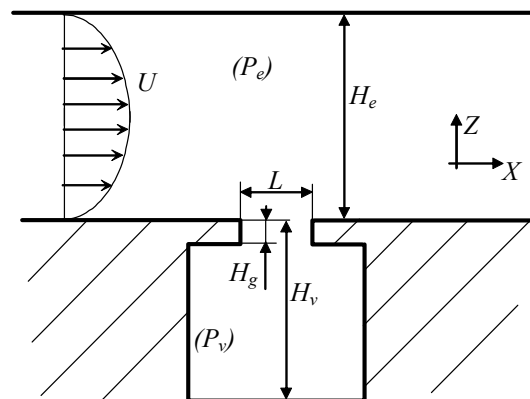


Figure 1. Configuration of the study

However, in order to be self-sustained, the shear layer oscillation has to interact with another system within a resonance effect. Flush-mounted cavities have been also well studied in the past, Naudascher & Rockwell (1994), Luca et al. (1995), Massenzio (1997) and Noger (1999) for examples. The case of rectangular cavities, and their tone frequencies has been reviewed and studied by Tam & Block (1978). Recently, the

resonance in piping systems has been investigated by Ziada & Shine (1999).

However, the resonance problem between an impinging shear layer and an acoustic mode of a pipe is not well documented. Moreover, the influence for instance of the incoming boundary layer thickness has only been reported by Sarohia (1977) in a non resonant configuration and requires more experiments and analysis.

The paper is organized as follows: first a deep cavity is studied, for which the resonance occurs not only with the duct but also with its volume. A shallow cavity, more common in piping systems, is studied with various variable parameters, especially the incoming boundary layer thickness and the neck thickness. Numerical simulations, by means of the commercial code Power Flow, are presented for the shallow cavity case.

NOMENCLATURE

A_c	section area of the neck
c_o	sound velocity
δ	boundary layer thickness
δl	displacement thickness
δl	momentum thickness
f_r	reduced frequency ($= fL / U_o$)
f_{sl}	frequency in the shear layer
f_t	mode frequency of the test section
f_v	cavity natural frequency
f	sound frequency
H_g	cavity neck depth
H_v	cavity total depth
L	cavity neck width
M	Mach number ($= U_o / c_o$)
P_{sl}	acoustic pressure in the shear layer
P_e	acoustic pressure outside cavity
P_v	acoustic pressure inside cavity
St	Strouhal number ($= f_{sl} L / U_o$)
U_o	freestream velocity
V	volume of the cavity

EXPERIMENTAL SETUP

The models of the cavities have been mounted in a small acoustic wind tunnel of the Institut Aérotechnique which generates a very low noise airflow. Details on the facility and the measurement system are available in (Hémon 2000). An original feature is that it allows to measure the outside acoustic pressure P_e for a given range of frequencies even when the wind is blowing: this kind of measurement is performed by intensimetry and is better detailed in part 2 of the paper.

The acquisition system is the PAK system provided by Müller-BBM for which measurement hardware is based on the VXI standard. The acquisition card is a 16 bits A/D converter equipped with direct signal processors for Fast Fourier Transform measurements. The frequency resolution was chosen to be 0.18 Hz for the deep cavity and 0.5 Hz for the shallow one. The acoustic pressure accuracy is typically of 1dB. The

reference freestream velocity U_o is measured with an accuracy of around 1%.

The pressure measurements are completed by velocity measurements using hot wire anemometry. Boundary layer probes (Type P15 provided by Dantec) were used. The constant temperature anemometer was calibrated using a non linear fitting curve and the resulting accuracy is of 5%. Acquisition and numerical processing were made using the PAK system. The probes are mounted on a small vertical displacement trail which has a position resolution of 0.1 mm.

THE DEEP CAVITY

Description of the model and incoming flow

The model of the cavity has been flush-mounted in a rectangular closed test section 260 mm high and 300 mm wide. Dimensions of the model are $H_g=5\text{mm}$, $L=20\text{mm}$ and $V=0.0039\text{m}^3$. The neck section A_c is 0.004m^2 and the spanwise dimension is 200 mm. The cavity is very deep, its height being $H_v=10 L$. All these dimensions have been chosen in order to obtain a resonance frequency inside the intensimetry measurement range of the setup, between 80 and 660 Hz for a wind velocity around 10 to 25 m/s.

The pressure P_v in the cavity is measured by a microphone. The resonance frequency of this deep cavity was measured without wind by using an acoustic source providing a white noise in the test section. The response of the cavity gave a natural frequency of 263 Hz (± 0.5) which is in relatively good agreement with the expected value using the classical theory of the Helmholtz resonator.

The first acoustic modes of the test section, which is rectangular, are listed in Table 1 and given by the formula

$$f_t = c_o / 2 a \quad (1)$$

where a is the length of the relevant dimension, vertical or lateral. We can see that a priori the cavity resonance is far from these values and should not interact with the test section. Furthermore, from experiments, we found a little difference with formula (1) which is probably due to the finite length of the test section. Indeed it creates non ideal boundary conditions although it is assumed for the theoretical values.

Direction	Vertical	Lateral
Deep cavity	660 Hz	572 Hz
Shallow cavity	1252 Hz	1072 Hz

Table 1. Frequencies of the first acoustic modes of the test sections

The incoming boundary layer profile was measured in detail and given in Figure 2 in dimensionless variables. The mean velocity and its root-mean-square (RMS) are given reduced by the mean flow rate velocity. The mean velocity profile outside the viscous sub-layer can be well fitted by a logarithmic profile, which is a typical characteristic of a fully developed, equilibrium, turbulent boundary layer, with zero

pressure gradient. The resulting integral thicknesses are $\delta l=4.5$ mm and $\delta 2=3.6$ mm. It is known that the parameter $\delta l/L$ is very important for the shear layer instability in the neck: its value here is 0.22 which is small enough to a priori allow an excitation by the first mode of the attached shear layer, Sarohia (1977).

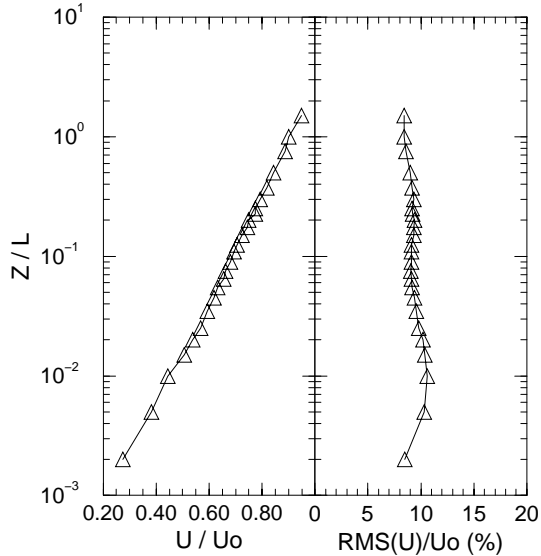


Figure 2. Boundary layer profile at X=-2 L for the deep cavity

Frequency and pressure level results

Figure 3 presents first the measured acoustic pressure level P_v inside the cavity, and secondly its corresponding frequency, versus the freestream velocity. The two sets of symbol correspond to the same test which was made twice. The physical unit for the pressure level is from a power spectral density and does not depend on the acquisition parameters. For a better approach of the physics, note that a pressure level of $25 Pa/\sqrt{Hz}$ is equivalent to 115 dB with our frequency resolution, which is a very high level for the human ear.

The horizontal dashed lines on the frequency curve are the frequencies which correspond to the natural frequency of the cavity, for the first one, and to one acoustic mode frequency of the test section for the second one. Each resonance case leads to a high pressure level in the cavity, and we focus the present paper on the second peak, which is the interaction with an acoustic mode of the test section.

Indeed, by observing the first series of measurements, we can see that the frequency is increasing quasi linearly with the wind velocity: then at a certain velocity, there is an emergence of a second tone in the spectrum which creates at 290 Hz a very high pressure level. In fact, the resonance is not really induced by this frequency but rather by its first harmonic which interacts with the lateral acoustic mode of the test section.

In order to verify that the lateral dimension of the test section was really the cause of the pressure peak, this dimension

was modified by adding a layer of wood on the lateral wall. Then, according to formula (1), the frequency was increased so that the resonance could not occur due to the limited range of the wind velocity. This was experimentally verified.

The second peak in the cavity response to the flow is a complex mechanism which is due to a coupling between the shear layer excitation, the volume of the cavity and an acoustic mode of the duct.

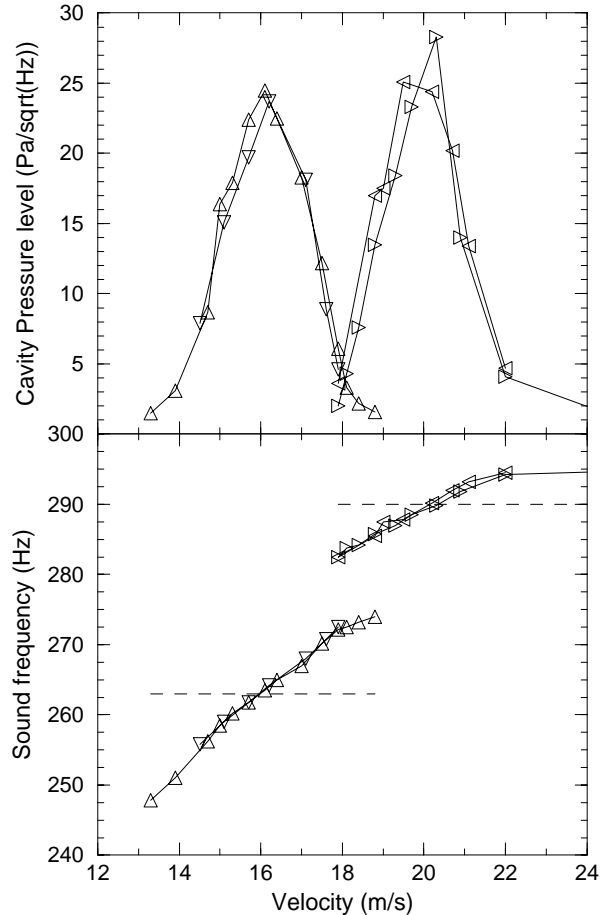


Figure 3. Cavity pressure level and corresponding frequency versus U_o for the deep cavity

Transfer function

In order to better understand the phenomenon, we measure using intensimetry the external pressure P_e , around the two resonance velocities. This is performed simultaneously with measurements of the internal pressure P_v . Then we plot the transfer function P_v/P_e in amplitude (modulus) and phase angle ϕ in Figure 4. The main point of these data is the phase angle which is found to be $97^\circ (\pm 2^\circ)$ at the resonance with the cavity for $U_o=16$ m/s. At the second point of resonance ($U_o=20$ m/s), the phase angle is very different (135°) and these differences should be physically interpreted.

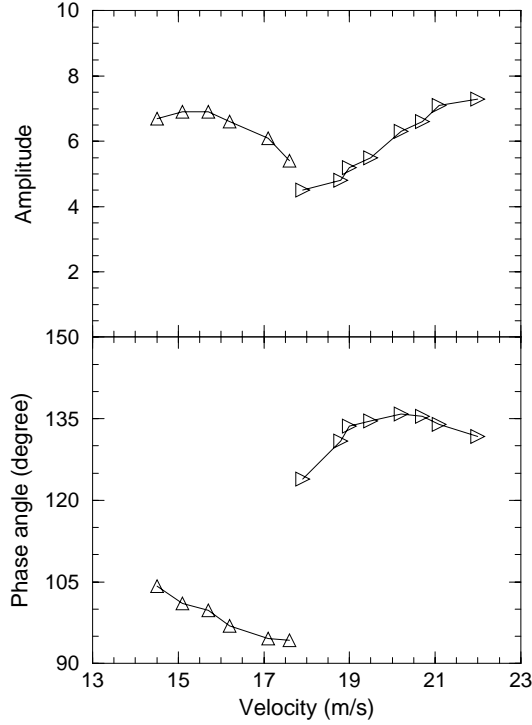


Figure 4. Transfer function P_v/P_e versus U_o for the deep cavity

From the classical theory of the Helmholtz resonator, assuming that the air is a perfect gas and the cavity is adiabatic, we may write

$$\frac{V H_g}{c_o^2 A_c} \ddot{P}_v + P_v = P_e + \varepsilon P_{st}. \quad (2)$$

The coefficient ε is a dimensionless unknown amplitude of the excitation term P_{st} produced in the neck by the shear layer instability. The external pressure P_e appears as a forcing term for the cavity pressure. Since the response is harmonic at resonance points, it may be written as

$$P_e = \alpha P_v + \beta \dot{P}_v. \quad (3)$$

This expression assumes linearity as a first approximation. Nevertheless, it must be recalled that the excitation is physically the instability of the shear layer, which is modelled by εP_{st} and can be estimated from the measurements of the other parameters of system (2). Indeed, this system has to be in equilibrium, i.e. at a zero balance of energy over one period. Then at resonance, the shear layer instability is tuned at the frequency of the cavity and the excitation term may be rewritten as

$$\varepsilon P_{st} = \mu \dot{P}_v. \quad (4)$$

By replacing (3) and (4) in (2) we can identify μ as

$$\mu = -\beta = \frac{1}{2\pi f} \left| \frac{P_e/P_v}{P_v/P_e} \right| \sin \phi, \quad (5)$$

and

$$\alpha = |P_e/P_v| \cos \phi, \quad (6)$$

where all the terms are measured and reported in Table 2. We see that the system is not only a simple resonator which is excited by a shear layer tuned in frequency. Indeed, the confinement of the flow above the cavity produces a damping which contributes to limit the pressure level in the cavity.

This damping is given by β and we can see that it is much smaller for the second peak: this is physically logical, the confinement being itself the cause of this resonance.

	First peak At $f_v=263$ Hz	Second peak At $f=290$ Hz
$\left \frac{P_v}{P_e} \right $	6.6	6.6
ϕ	97°	135°
α	$-1.85 \cdot 10^{-2}$	-0.107
$\beta = -\mu$	$-9.1 \cdot 10^{-5}$	$-5.9 \cdot 10^{-5}$

Table 2. Measured parameters of the system

Moreover, the coefficient of added stiffness α is much larger for the resonance involving the test section, which is again logical from a physical point of view. It explains also why the frequency of the second peak is higher than the natural cavity resonance, since the total stiffness is increased by 10.7%. This leads to a square root increase in frequency, which agrees with the measured frequency of the second peak (within an uncertainty range).

THE SHALLOW CAVITY

Description of the model and incoming flow

The shallow cavity is mounted in the same way as the deep one, behind a test section 160 mm wide and 137 mm high. The purpose of this smaller section is to be able to increase the velocity according to the capabilities of the setup in terms of flow rate. Expected Mach numbers are in the range [0.10 – 0.25].

The cavity dimensions in mm are $L=50$, $H_v=20$, and 150 spanwise. The neck thickness H_g is variable, between 2 to 8 mm. The neck section is $A_c=0.0075$ m² and the volume is $V=0.00013$ m³. From experience, it is not expected here to obtain an excitation of the cavity volume by the shear layer, as in a Helmholtz resonator.

However, a resonance between the shear layer frequency and the vertical acoustic mode of the test section, given in Table 1, is expected. The dimensionless frequencies of the oscillations of the shear layer are well approximated by Rossiter's formula (1964)

$$St = \frac{n - \gamma}{M + U_o/U_c}, \quad (7)$$

where n is the order of the mode and γ a parameter linked to the shape of the lips and usually equal to 0.25 for sharp edges and rectangular cavities (see Tam & Block (1978) for a review). The

ratio of the convection velocity U_c to the freestream velocity U_o is almost universal and equal to 0.57.

Nevertheless, it was shown by Sarohia (1977) that the incoming boundary layer thickness was an important parameter of such a problem, even if his study is not completely transposable to ours. His experiments showed that a small boundary layer thickness (usually reduced by the neck length) is able to induce the shear layer oscillations on the first mode ($n=1$ in Rossiter's formula), although a larger thickness is exciting the higher orders. Anyhow in the present study, the model of the cavity and its associated test section are designed in order to reach a frequency range of resonance corresponding to the second order mode of Rossiter ($n=2$).

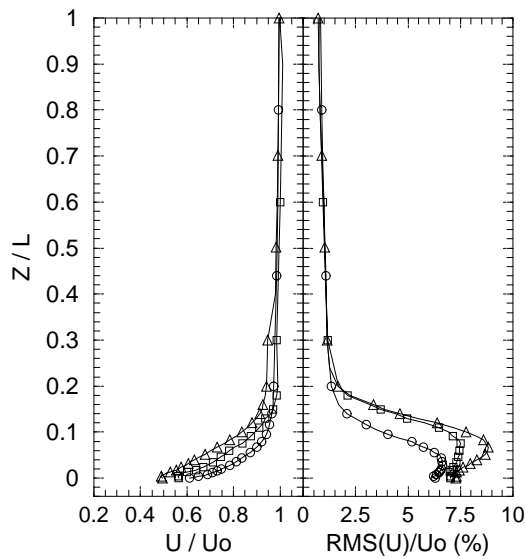


Figure 5. Boundary layer profiles for the shallow cavity. ○: Smooth wall, □: Roughness 1, △: Roughness 2

	$\delta 1$ (mm)	$\delta 2$ (mm)	$\delta 1/L$
Smooth wall	1.42	1.26	0.0284
Roughness 1	1.65	1.26	0.0330
Roughness 2	2.94	2.25	0.0588

Table 3. Integral thicknesses of the boundary layers for the shallow cavity

The measured boundary layer profiles 5 mm upstream the shallow cavity are given in Figure 5. The vertical origin is the wall of the tunnel. The smooth wall case leads to a boundary layer at equilibrium. Some roughnesses, consisting in glued sand paper sheets, are used in order to increase the thickness. These two cases create thicker boundary layers which are not at equilibrium, as can be seen on the mean velocity profiles. The integral thicknesses for the three cases are given in Table 3. The second roughness leads to a thickness doubled compared to the smooth wall.

Mach number effect

Figure 6 presents the acoustic pressure level inside the cavity and the corresponding frequency for the main observed peak, versus the Mach number. The two extreme cases of neck thickness are shown, the smallest one leading to a very high pressure level.

In order to compare our results with Rossiter's formula, we give in Figure 7 the dimensionless frequency corresponding to the results in Figure 6. The lock-in of the shear layer oscillation with the acoustic mode of the test section is clearly visible. The dot-dashed line corresponds to the original Rossiter's formula and the dashed line to the acoustic vertical mode.

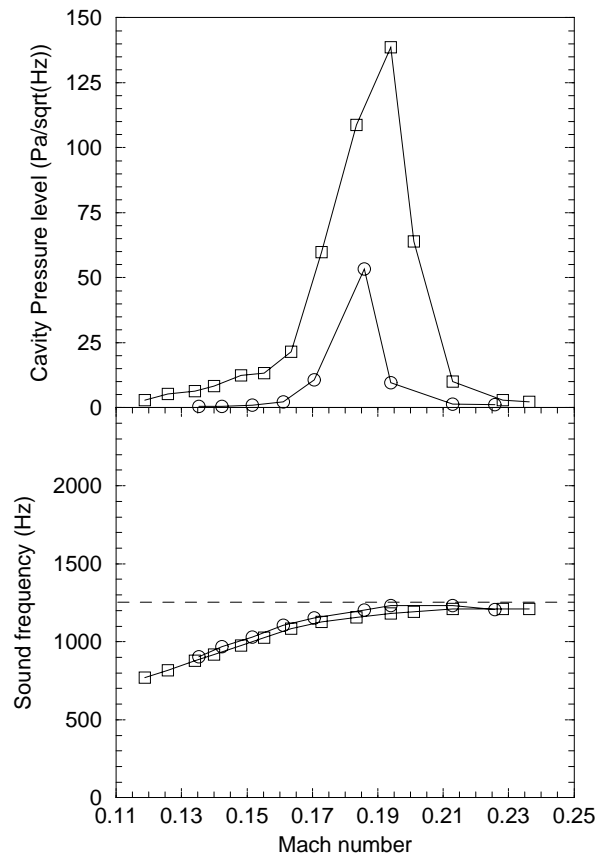


Figure 6. Cavity pressure level and corresponding frequency versus M for the shallow cavity
□: $H_g=2\text{mm}$, ○: $H_g=8\text{mm}$

These results in frequency are relatively in good agreement with Rossiter's formula. Measurements give larger Strouhal numbers which are in agreement with those of Tam & Block (1978) for the low Mach number range of the study. At lock-in, the velocity profiles in the shear layer are given in Figure 8 and 9 for the longitudinal positions $L/2$ and $0.88 L$ respectively. The profile of the velocity Power Spectral Density (PSD) at the resonance frequency is also given. The velocity oscillations are very large even at a relatively high level above the neck, and its spatial amplitude is growing along the longitudinal axis.

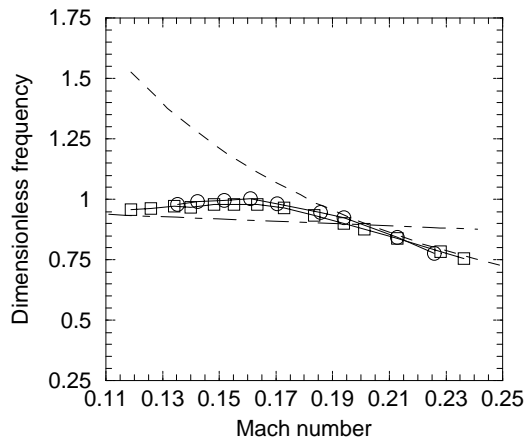


Figure 7. Dimensionless frequencies versus M for the shallow cavity. \square : $H_g=2\text{mm}$, \circ : $H_g=8\text{mm}$

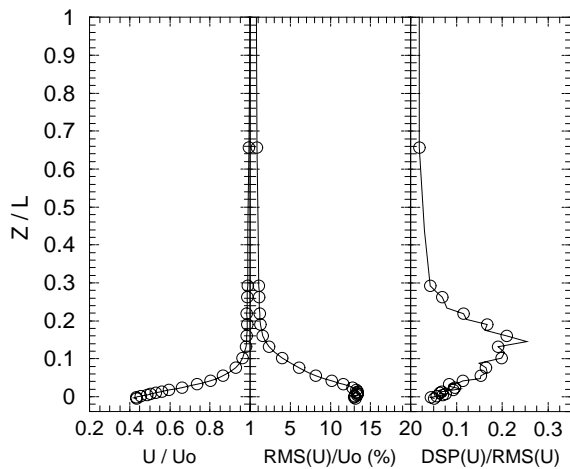


Figure 8. Shear layer velocity profiles for the shallow cavity with $H_g=8\text{mm}$ at $M=0.187$ and mid-length of the neck

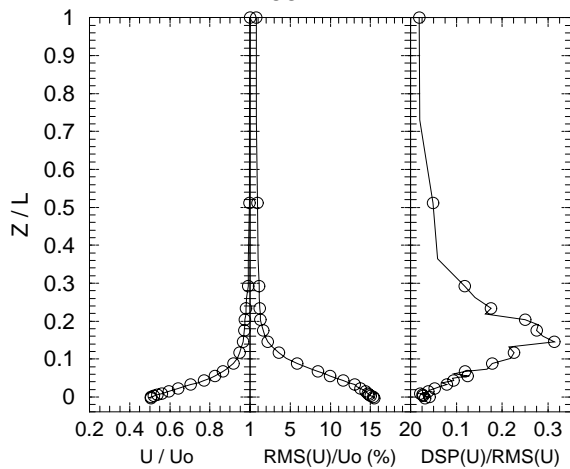


Figure 9. Shear layer velocity profiles for the shallow cavity with $H_g=8\text{mm}$ at $M=0.187$ and streamwise position $0.88 L$ from upstream lip

Influence of the boundary layer thickness

The influence of the boundary layer thickness is reported in Figure 10 where we have plotted the main peak (pressure level and corresponding frequency) versus the displacement thickness. The thicker boundary layers lead to a large decrease of the sound level.

However, from a physical point of view, this parameter should be associated to the total thickness of the shear layer which is located at the upstream lip of the cavity: the neck thickness H_g is an important part of it. Its influence is given in Figure 11 for the minimum value of 2 mm up to 8 mm which is the standard configuration.

Nevertheless, the effective total thickness of the shear layer is closer to an equivalent H_g given by $H_{geq}=H_g+\delta l$: all the previous results are then collected together in Figure 12. The isolated star symbol corresponds to a test with $H_g=2$ mm and roughness 1. There is a critical value around $H_{geq} = 9.5$ mm which leads to a strong decrease, close to cancellation, of the resonance peak. This critical value was also detected by Sarohia (1977) who noticed that no cavity oscillations occur when L/H_{geq} is below 5.25 (one has $L=50$ mm here), even for a cavity configuration which differs from ours.

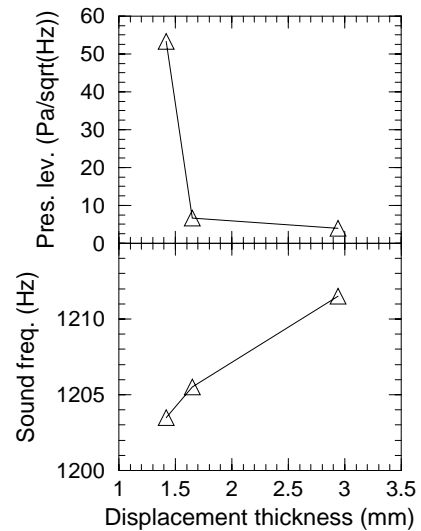


Figure 10. Maximum pressure levels and corresponding frequencies versus δl for the shallow cavity with $H_g=8\text{mm}$

A second critical value is around $H_{geq} = 5$ mm ($L/H_{geq} = 10$) below (resp. above) which the sound level is significantly increased, whereas it is almost constant for H_{geq} between 5 to 9.5 mm. Although it is less obvious with the additional test (star symbol), its level is however increased also. This second critical value requires further investigations to better understand the reason of this jump.

It may also be noticed that there exists an increase of the frequency oscillation with this parameter, the slope of which (using a linear least square approximation) is 5 Hz/mm. This

leads to an increase of the Strouhal number according to formula

$$St = 0.20 \frac{H_{geq}}{L} + St_o, \quad (8)$$

where $St_o = 0.93$ corresponds to the dimensionless frequency obtained for a zero thickness.

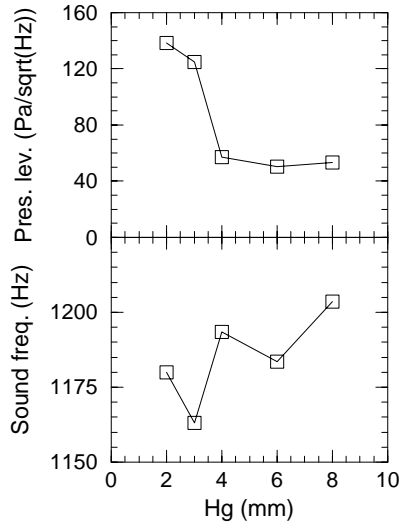


Figure 11. Maximum pressure levels and corresponding frequencies versus H_g for the shallow cavity with the small boundary layer thickness

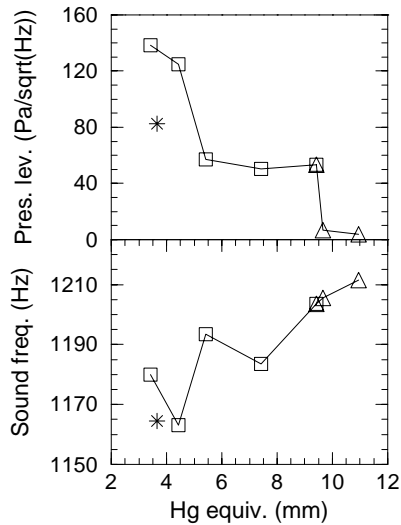


Figure 12. Maximum pressure levels and corresponding frequencies versus $H_g + \delta l$ for the shallow cavity

Sound attenuation

We have seen above that the increase of the boundary layer thickness is a very good way for sound attenuation. In a piping system a great disadvantage of this is the increase of the pressure loss. Addition of a deflector just upstream would have

the same effect. Other solutions have therefore been explored: the problem is that the modifications that can be performed are generally limited by the kinematics of the valve for example.

Since the shear layer oscillation is due to a series of vortex rolls which are quasi two-dimensional at resonance, a spanwise decrease of the vortex correlation should reduce the resonant excitation. Figure 13 presents a design of crenels made on the upstream lip. Their width is 5 mm, with a distance of 20 mm between their axis; the resulting configuration is called “crenels $\frac{1}{4}$ ” (5 mm over 20 mm). Another configuration has been implemented, called “crenels $\frac{1}{2}$ ” which have crenels 10 mm wide. The third tested solution was the “right crenels $\frac{1}{4}$ ” which have the same size of the “crenels $\frac{1}{4}$ ” but with a sectional shape forming a backward facing step instead of a 45° bevel edge.

The results of the tests are given in Table 4 where only the maximum pressure level is given. The “crenels $\frac{1}{4}$ ” have almost the same efficiency as the “crenels $\frac{1}{2}$ ”. It is interesting to see that the shape of the crenels is important, since the “right crenels $\frac{1}{4}$ ” produce a significant attenuation, the pressure being divided by a factor larger than 3.

Configuration	Pressure level (Pa / \sqrt{Hz})
Standard	53.3
Crenels $\frac{1}{4}$	23.0
Crenels $\frac{1}{2}$	23.5
Right crenels $\frac{1}{4}$	15.9

Table 4. Maximum pressure levels with sound attenuation systems, for the shallow cavity with $H_g=8\text{mm}$ and small boundary layer

Numerical simulations

Numerical simulations of the shallow cavity have been carried out, using Exa’s Power Flow commercial code. The simulated configuration corresponds to the 8 mm neck thickness with the small boundary layer.

Power Flow

Power Flow uses a lattice gas method, Chen *et al.* (1997), which is a particle-based method. The basic theoretical difference between this method and traditional Computational Fluid Dynamics is that it simulates a discrete fluid, while other methods solve discretized partial differential equations, typically the Navier-Stokes equations. It tracks the motion of macromolecules through space and time to physically simulate the flow. It inherently conserves mass, momentum and energy. The particles exist at discrete locations in space, moving in discrete directions with discrete speeds at discrete intervals of time. The particles reside on a cubic lattice with symmetry properties necessary for artifact-free simulation. They move from the center of one element to the center of another at each time step. Every time step consists of two separate phases: move and collide.

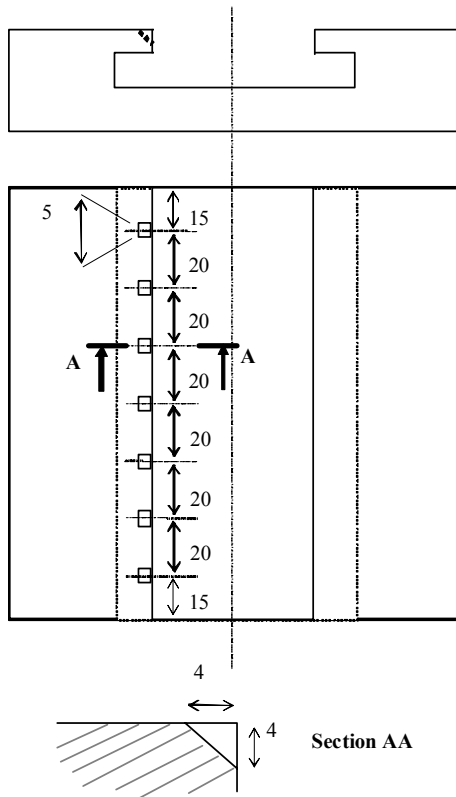


Figure 13. Upstream lip modification for sound attenuation, “crenels ¼”

Characteristics of the simulation

In this study, we used the Very Large Eddy Simulation prediction of turbulence proposed by Power Flow, which uses a k-ε RNG model and a wall law. The velocity at the inlet of the duct is imposed in order to adjust the desired Mach number.

A 0.012 m diameter microphone probe is placed at the centre of the cavity bottom. When it is activated, it records the pressure for each time step (sampling frequency of about $8.58 \cdot 10^5$ Hz). For each case, the pressure is recorded after the time necessary for the initialization of the mechanisms. The records last about 0.6 second, which corresponds to several hundreds periods of the interesting pressure fluctuations.

The simulations are performed in 2D. The geometry of the cavity is exactly the same as in the experiments. The upstream length has been adjusted in order to obtain the same boundary layer parameters. These values are given in Table 5 and compared to the experimental ones.

Results

The evolution of vorticity is presented in Figure 14 for a Mach number 0.17 (at lock-in). The time interval between each image is set to give 4 images per cycle with a frequency of 1200 Hz. It is clear that there is a vortex which periodically impacts the downstream edge of the cavity.

The dimensionless frequencies of the test section acoustic mode, the Rossiter’s formula and the numerical results, as well

as the pressure level are presented in Figure 15 versus Mach number. The observations are close to the experimental ones:

- the shear layer oscillation mode is generated, it corresponds to Rossiter’s mode 2,
- for Mach numbers between 0.17 and 0.21, this mode is locked-in with the acoustic mode of the duct, giving rise to a distinct increase in the pressure level.
- The pressure level associated to mode 2 increases then decreases with Mach number. The maximum pressure level corresponds to Mach number around 0.195.
- The acoustic mode of the duct is detected, whatever the Mach number.

Figure 16 presents a comparison of the experimental and numerical signals, for a Mach number corresponding to the maximum pressure level during lock-in (i.e. 0.183 experimentally and 0.195 numerically). The two lock-in frequencies are very close. The numerical signal is sharper than the experimental one and the pressure level seems over-estimated. This might be due to the ideal configuration of the numerical simulations: pure resonance, no wall absorption and 2D simulations.

	δ_1 (mm)	δ_2 (mm)	δ_1/δ_2
numerical	1.45	1.19	1.22
experimental	1.42	1.26	1.13

Table 5. Boundary layer parameters

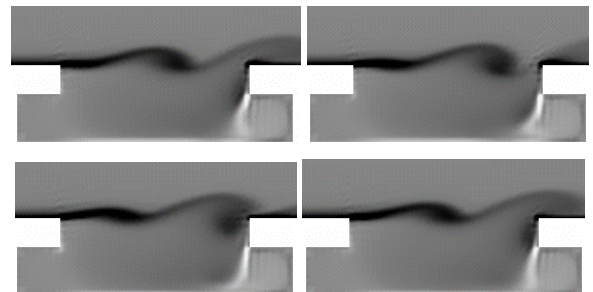


Figure 14. Vorticity field evolution in time, $M = 0.17$

Conclusions on numerical simulations

The numerical study of the shallow cavity using Power Flow showed that this code can reproduce correctly the evolution of the shear layer fluid instability at the neck of the cavity with Mach number. The lock-in of this instability with an acoustic mode of the duct was also reproduced.

Rossiter’s mode 2, the test section acoustic mode and their lock-in for Mach numbers between 0.17 and 0.21 are well detected. The evolution of the acoustic pressure levels of the peaks is roughly in accordance with the experimental results.

Only the values of pressure levels are overestimated compared to the experimental values, due to the ideal configuration in which the simulation occurs.

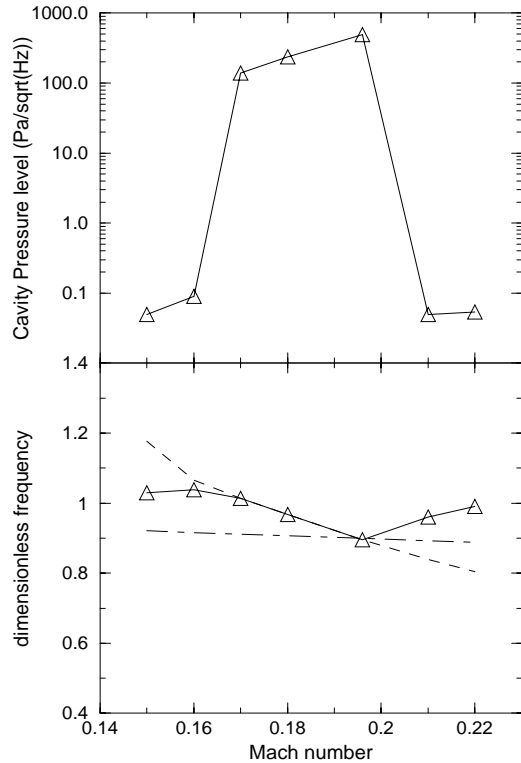


Figure 15. Dimensionless frequency and pressure level versus Mach number. -----: acoustic mode, - · - · - : Rossiter's formula, Δ : numerical results

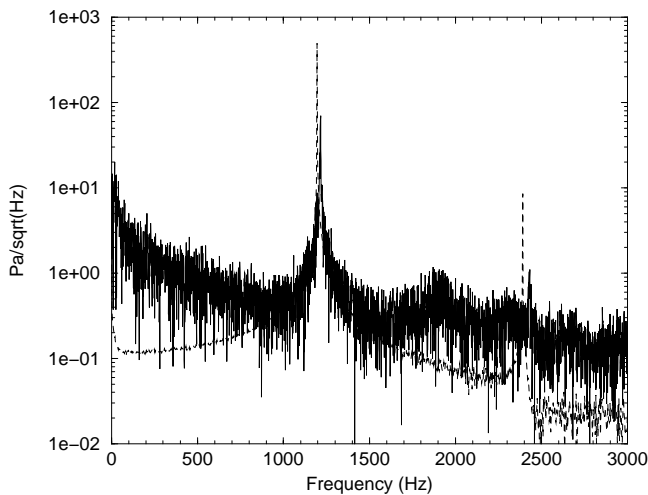


Figure 16. Comparison of experimental and numerical signals

CONCLUSION

Experiments have been presented concerning the interaction of the shear layer created by confined flows over cavities with a pipe acoustic mode. The application lies in the sound generated in piping systems due to singularities such as valves.

The cases of a deep and a shallow cavity have been tested, the first one being close to a so-called Helmholtz resonator. It was shown by measurements that the added damping due to the confinement is smaller when the resonance occurs with the duct, than when the resonance occurs classically with the Helmholtz resonator.

The shallow cavity was studied in a parametric way versus the boundary layer and neck thicknesses. Critical values have been detected but further investigations have to be performed and analyzed. A few passive sound attenuation techniques have also been explored. Moreover, numerical simulations using a lattice gas method have presented results qualitatively in accordance with the experiments.

ACKNOWLEDGMENTS

The study of the shallow cavity was performed at the Institut Aérotechnique in association with the department of Analysis in Mechanics and Acoustics of Electricité de France, within the research contract No E27312.

REFERENCES

- CHEN H., TEIXEIRA C. & MOLVING K. Digital Physics approach to Computational Fluid Dynamics: some basic theoretical features. *International Journal of Modern Physics C*, **8**(4) (1997).
- HEMON P., AMANDOLESE X., SANTI F & WOJCIECHOWSKI J. Study of the acoustic oscillations by flows over cavities. Part 2. Sound reduction. *5th International Symposium on FSI*, New Orleans, 17-22 November (2002), paper No NCA-33376.
- HEMON P. Mesure des caractéristiques acoustiques de singularités aérauliques en présence de l'écoulement. SIA Colloquium on « Confort automobile et ferroviaire », Le Mans, 15 & 16 novembre (2000), paper No CAF/00-28 (in french).
- HO C-M & HUERRE P. Perturbed free shear layers. *Annual Review of Fluid Mechanics* **16** (1984) 365-425.
- LUCA M.J. et al. The Acoustic Characteristics of Turbomachinery Cavities. NASA CR 4671, (1995).
- MASSENZIO M. Caractérisation des sources aéroacoustiques sur trains grande vitesse en vue de la prévision de la pression acoustique interne. Thesis of INSA Lyon, (1997).
- NAUDASCHER E. & ROCKWELL D. Flow-induced vibrations. Balkema, Rotterdam, (1994).
- NOGER C. Contribution à l'étude des phénomènes aéroacoustiques se développant dans la baignoire et autour des pantographes du TGV. Thesis of Université de Poitiers, (1999).
- ROCKWELL Donald. Oscillations of Impinging Shear Layers. *Journal of AIAA*, **21**(5) (1983) 645-664.
- ROSSITER J.E. Wind tunnel experiments on the flow over rectangular cavities at subsonic and transonic speed. *Aero. Res. Counc. R. & M.*, No. 3438 (1964).
- SAROHIA V. Experimental investigation of oscillations in flows over shallow cavities. *Journal of AIAA*, **15**(7) (1977) 984-991.

TAM C.K.W. & BLOCK P.J.W. On the tones and pressure oscillations induced by flow over rectangular cavities. *Journal of Fluid Mechanics* **89** (1978) 373-399.

ZIADA S. & ROCKWELL D. Oscillations of an unstable mixing layer impinging upon an edge. *Journal of Fluid Mechanics* **124** (1982) 307-334.

ZIADA S. & SHINE S. Strouhal numbers of flow-excited acoustic resonance of closed side branches. *Journal of Fluids and Structures* **13** (1999) 127-142.